



ELSEVIER

Contents lists available at ScienceDirect

Plant Physiology and Biochemistry

journal homepage: www.elsevier.com/locate/plaphy

Research article

Highlight on the expression and the function of a novel MnSOD from diploid wheat (*T. monococcum*) in response to abiotic stress and heavy metal toxicitySana Tounsi^a, Kaouther Feki^b, Yosra Kamoun^c, Mohamed Najib Saïdi^a, Sonia Jemli^d, Mouna Ghorbel^a, Carine Alcon^e, Faiçal Brini^{a,*}^a Biotechnology and Plant Improvement Laboratory, Centre of Biotechnology of Sfax (CBS)/University of Sfax, B.P "1177", 3018, Sfax, Tunisia^b Laboratory of Legumes, Centre of Biotechnology Bordj Cedria, BP 901, 2050, Hammam Lif, Tunisia^c Laboratory of Molecular Biotechnology of Eukaryotes, Centre of Biotechnology of Sfax, B.P "1177", 3018, Sfax, Tunisia^d Laboratory of Microbial Biotechnology and Enzymes Engineering, Centre of Biotechnology of Sfax, B.P "1177", 3018, Sfax, Tunisia^e Biochimie & Physiologie Moléculaire des plantes, PHIV platform, UMR 5004 CNRS/386 INRA/Supagro Montpellier / Université Montpellier 2, Campus Supagro-INRA, 34060, Montpellier Cedex 2, France

ARTICLE INFO

Keywords:

Triticum monococcum
MnSOD
Abiotic stress
Heavy metals
Tolerance

ABSTRACT

Superoxide dismutases (SODs) play a pivotal role in improving abiotic stress tolerance in plant cells. A novel manganese superoxide dismutase gene, denoted as *TmMnSOD*, was identified from *Triticum monococcum*. The encoded protein displayed high sequence identity with MnSOD family members and was highly homologous to TdMnSOD from durum wheat. Furthermore, the 3D structure analysis revealed that TmMnSOD displayed homotetramer subunit organization, incorporating four Mn²⁺ ions. Notably, TmMnSOD structure contains predominantly alpha helices with three beta sheets. On the other hand, under stress conditions, *TmMnSOD* transcript level was significantly up-regulated by salt, oxidative and heavy metal stresses. At the functional level, *TmMnSOD* imparts tolerance of yeast and *E. coli* cells under diverse stresses. Promoter analysis of *TmMnSOD* gene showed the presence of a great number of salt and pathogen-responsive *cis*-regulatory elements, highlighting the interest of this gene in breeding programs towards improved tolerance to salt stress in wheat.

1. Introduction

Superoxide dismutases play crucial role in protecting plant cells from oxidative stress, which is generated during metabolic processes and under various environmental conditions. SODs are considered as the first barrier of cellular defense against reactive oxygen species (ROS), catalyzing the dismutation of superoxide radical anions to hydrogen peroxide (H₂O₂) and oxygen (O₂) (Del Rio et al., 2003; Gill and Tuteja, 2010; Mhamdi et al., 2010). Based on their metal cofactor interacting with their active sites, plant SODs are divided into three groups including iron SOD (FeSOD), copper–zinc SOD (Cu/ZnSOD) and manganese SOD (MnSOD) (Zhang et al., 2016a,b; Zhou et al., 2017). Each SOD group displays a diverse subcellular localization and structural features in plants (Alscher et al., 2002; Zhang et al., 2016a,b). Cu/ZnSODs and FeSODs are predominately found in chloroplast and cytosol, while MnSODs are mainly located in mitochondria (Gill and Tuteja, 2010; Miller, 2012). Comparison of amino acid sequences from these different SODs suggest that Mn and Fe SODs are considered as the ancient types of SODs, which probably evolved from the same ancestral

enzyme, whereas Cu/ZnSODs sequences are different from Mn and FeSODs and probably have evolved separately in eukaryotes (Dehury et al., 2012a,b).

In recent years, several SODs genes were identified from various plant species such as *Arabidopsis* (Kliebenstein et al., 2010; Yadav et al., 2018), *Medicago truncatula* (Song et al., 2018), *Sorghum bicolor* (Filiz and Tombuloglu, 2015), cotton (Zhang et al., 2016a,b), rice (Nath et al., 2014; Yadav et al., 2018) and wheat (Feki et al., 2016; Wang et al., 2016; Tyagi et al., 2017). Genome wide analysis revealed that the numbers of SOD genes in *Arabidopsis*, rice, *Sorghum* and bread wheat are 8 (4 Cu/ZnSODs, 2 FeSODs and 2 MnSODs), 8 (5 Cu/ZnSODs, 2 FeSODs and 1 MnSOD), 8 (5 Cu/ZnSODs, 2 FeSODs and 1 MnSOD) and 23 (14 Cu/ZnSODs, 6 FeSODs and 3 MnSODs), respectively. The number of these genes varied among plant species and Cu/ZnSODs were considered as the most predominant members compared to FeSODs and MnSODs (Gill and Tuteja, 2010; Gill et al., 2015; Verma et al., 2019).

Transcript profiling of SOD family from several plant species revealed that they play crucial role in scavenging ROS generated during plant growth and in response to various abiotic stresses. Their

* Corresponding author.

E-mail address: faical.brini@cbs.rnrt.tn (F. Brini).<https://doi.org/10.1016/j.plaphy.2019.08.001>

Received 14 May 2019; Received in revised form 9 July 2019; Accepted 2 August 2019

Available online 02 August 2019

0981-9428/ © 2019 Elsevier Masson SAS. All rights reserved.

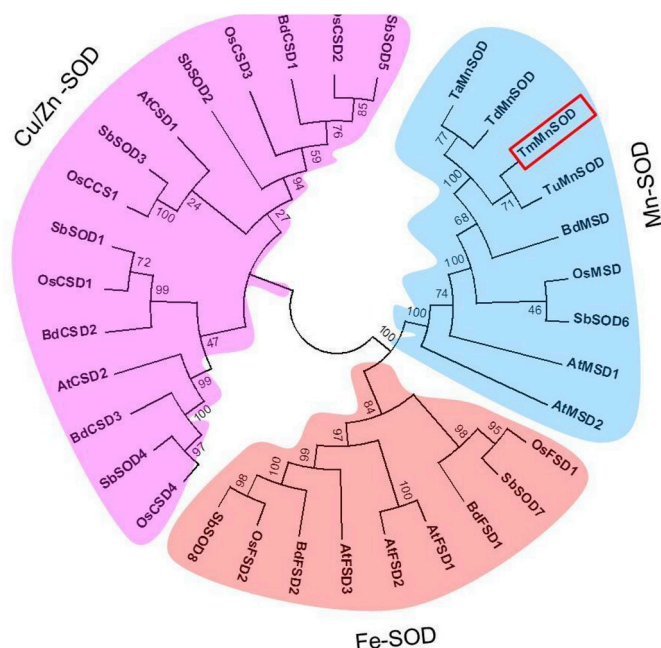


Fig. 1. Phylogenetic analysis of TmMnSOD with other plant SODs proteins. (A) The phylogenetic tree was constructed using the Neighbor-Joining method with 1000 bootstrap replicates, based on amino acid sequences from phytosome, gramene and NCBI databases. Wheat, *B. distachyon*, rice, *Sorghum bicolor*, and *Arabidopsis* identifiers are illustrated in [Supplementary Table S1](#). Tm *Triticum monococcum*, Td *Triticum turgidum* subsp. durum, Ta *Triticum urartu*, Bd *Brachypodium distachyon*, Os *Oryza sativa*, Sb *Sorghum bicolor*, At *Arabidopsis thaliana*.

expression was regulated by salt, oxidative, drought, cold, heat and heavy metal stresses (Khan et al., 2007; Gill et al., 2015; Yadav et al., 2018). Expression analysis of different SOD genes from rice (*OsCu/ZnSOD4*, *OsFeSOD1* and *OsMnSOD*) and *Arabidopsis* (*AtCu/ZnSOD2*, *AtMnSOD1* and *AtFeSOD1*) revealed that they are up-regulated by various environmental conditions such as salt, drought, cold and heat (Yadav et al., 2018). However, most SOD genes from *M. truncatula* were shown to be down-regulated under salt and drought stresses (Song et al., 2018). In cucumber, all CsSOD genes showed significant up-regulated expression under heat treatment. Whereas, under salt stress CsCSD2 was the only gene that showed increased expression level, suggesting a potential role of CsCSD2 in response to salt stress (Zhou et al., 2017). In barley, heat stress had no significant impact on *HvCu/ZnSOD* expression however its expression was induced by drought, cold, H₂O₂ and MV treatments (Abu Romman and Shatnawi, 2010).

The bread wheat genome contained several SODs genes with diverse expression patterns and functions in response to biotic and abiotic stresses (Tyagi et al., 2017). The role of wheat SOD genes in abiotic stress response has been well studied. It was reported that transgenic tobacco plants overexpressing TaSOD1.1 and TaSOD1.2 have better tolerance to salt stress (Zhang et al., 2008). Furthermore, recent study showed that overexpression of a wheat Cu/ZnSOD2 (TaSOD2) improved tolerance to salt and oxidative stresses in both transgenic wheat and *Arabidopsis* plants (Wang et al., 2016). Three MnSOD genes were reported to be present in bread wheat genome (Kumar et al., 2013; Tyagi et al., 2017). Only one MnSOD gene has been isolated and characterized from bread wheat (Kumar et al., 2013) and durum wheat

(Feki et al., 2016). However, no SOD gene in the diploid wheat (*T. monococcum*) has been reported so far.

In the current study, we report the functional characterization of a novel *TmMnSOD* gene from *T. monococcum*. We analyzed and compared its functional domains, genomic organization and sequence homology with other MnSODs. In addition, we studied its expression pattern under different stresses. Moreover, we assessed the function of *TmMnSOD* in response of yeast and *E. coli* cells to various environmental conditions.

2. Materials and methods

2.1. Plant material and growth conditions

Seeds of *Triticum monococcum* (cv. Turkey) Seeds of *T. monococcum* (cv. Turkey) and *T. turgidum* (cv. Om Rabia3) were provided by the ICARDA (Genetic resources Unit, Syria) and INRAT (Laboratoire de Physiologie Végétale, Tunisia), respectively. Seeds were surface sterilized as described by Tounsi et al., (2019) and grown in growth chamber under 16 h light/8 h dark cycles at 23 °C. Seven days after germination, seedlings were transferred onto half-strength Hoagland hydroponic solution (Davenport et al., 2005).

2.2. Molecular cloning of TmMnSOD from T. monococcum

The Full-Length *TmMnSOD* cDNA was isolated from *T. monococcum* using two specific primers SOD-F (5'-TAGGATCCATGGCGCTCCGCAC GTTGGCCGCG-3', BamHI site underlined) and SOD-R (5'-AGGAATTC CGAAGCACTTTTCATACTCTT- 3', EcoRI site underlined), designed based on *TdMnSOD* sequence (accession no. KP696754). The 3'-end of *TmMnSOD* was verified using the primers SOD-F and oligo-dT and the 5' region was isolated using the HE-TAIL-PCR method as described below. PCR products were purified from agarose gel, cloned in pGEM-T easy vector, and sequenced using ABI PRISM automated sequencer.

2.3. Expression analysis of TmMnSOD by real time PCR

For transcript analysis, Two-weeks-old plants were treated with 100 mM NaCl, 10 mM H₂O₂, 15% PEG (w/v), 100 μM ABA and 100 μM CdCl₂ for 24 h and 72 h. Total RNA was isolated from frozen tissue (roots and leaves) using Trizol method (Invitrogen) and cDNA was prepared using M-MLV reverse transcriptase (Invitrogen) in accordance with the manufacturer's recommendations. Primers were designed with Primer 3 software for *TmMnSOD* and *actin* genes using following gene-specific primers for *TmMnSOD*, qTmMnSOD-F (5'-GCCATTGATGAGG ATTTTGG-3') and qTmMnSOD-R (5'-CCAAGCTAGCCACCCATC-3') and for *actin*, qACT-F (5'-TGCATAGAGGGAAAGCACG-3') and qACT-R (5'-AACCCAAAAGCCAACAGAGA-3'). qPCR analysis was performed as previously described by Tounsi et al. (2019). The relative expression level was calculated based on the comparative CT method with the *actin* gene as an internal expression standard using formula $2^{-\Delta\Delta CT}$ (Livak and Schmittgen, 2001).

2.4. In silico analysis

Sequence analysis, functional domain and gene structure were performed as previously described by Tounsi et al., (2019). The conserved motifs of MnSOD proteins from wheat, *Brachypodium distachyon*, *Sorghum bicolor* and *Arabidopsis thaliana* were detected using MEME (<http://meme-suite.org/>). A predicted subcellular localization of TmMnSOD protein was determined using CELLO prediction tool

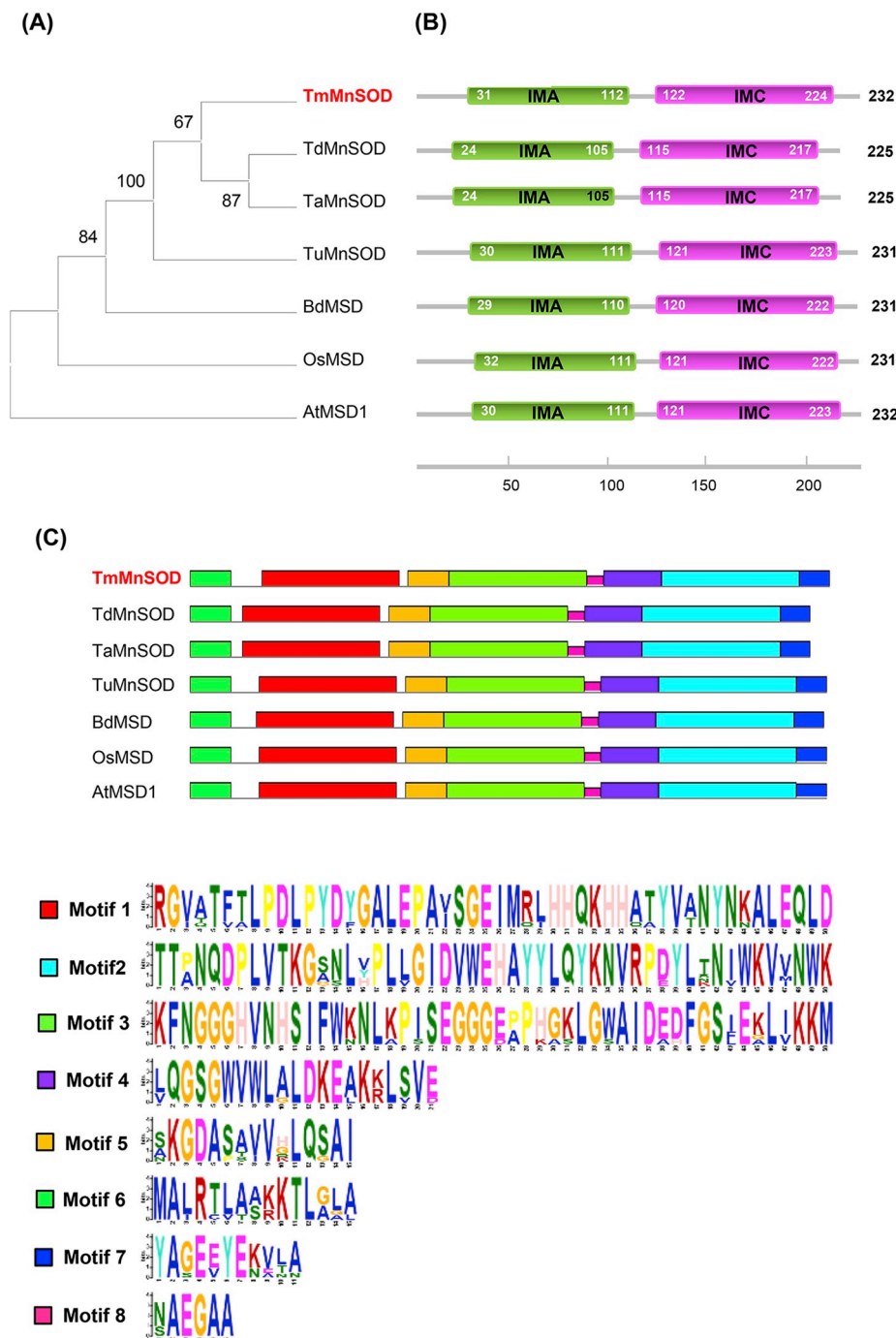


Fig. 2. Phylogenetic analysis, functional domains and conserved motifs of TmMnSOD and other MnSOD from wheat, *Brachypodium*, rice and *Arabidopsis*. (A) Phylogenetic tree of TmMnSOD and their homologs from wheat, *Brachypodium*, rice and *Arabidopsis* (Supplementary Table S1). (B) Functional domains analysis of MnSODs proteins using InterPro and Pfam tools. The iron/manganese superoxide dismutase alpha-hairpin domain (IMA) and iron/manganese superoxide dismutase C-terminal domain (IMC) are highly conserved in all MnSODs proteins. (C) The conserved motifs of MnSODs proteins were identified by MEME. Each motif is represented with a specific color. (For interpretation of the references to color in this figure legend, the reader is referred to the Web version of this article.)

(<http://cello.life.nctu.edu.tw/>). The automated protein structure homology modeling server, Swiss Model (<http://www.expasy.org/swissmod/>), was used to generate the three-dimensional structural model of TmMnSOD using the crystal structure of manganese superoxide dismutase from *Arabidopsis thaliana* as template (PDB code 4C7U) (Marques et al., 2014). The model was therefore evaluated and validated by Ramachandran plots using the online tool RAMPAGE (<http://mordred.bioc.cam.ac.uk/~rapper/rampage.php>). The PyMOL v0.99 program (<http://www.pymol.org>) was used to visualize and analyze the generated model structure and to construct graphical presentations and illustrative figures. The search for *cis*-regulatory elements on the

promoter region of *TmMnSOD* and *TdMnSOD* genes was performed using PLACE (<http://www.dna.affrc.go.jp/PLACE/signalscan.htmlUH>) and PlantCARE (<http://bioinformatics.psb.ugent.be/webtools/plantcare/htmlUH>) databases (Higo et al., 1999; Lescot et al., 2002). For statistical analysis, the one way ANOVA was performed using the SPSS ver.13 statistical package. Significant means were indicated by different alphabets.

2.5. Heterologous expression of *TmMnSOD* in yeast cells

The full-length cDNA of *TmMnSOD* was inserted in the pYES2 vector

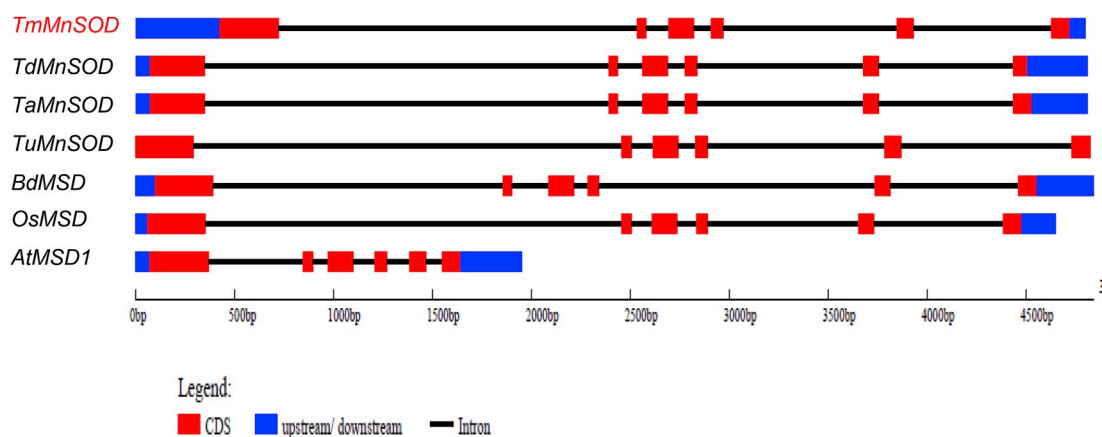


Fig. 3. Gene structure analysis of *TmMnSOD* and other *MnSODs* genes from wheat, *Brachypodium*, rice and *Arabidopsis* using GSDS tool.

using the *Bam*HI/*Eco*RI restriction enzymes. The PEG lithium acetate transformation method (Gietz et al., 1995) was carried out in order to transfer the recombinant plasmid pYES2-*TmMnSOD* and the empty vector into *S.cerevisiae*, W303.1A (*MATa ade2 ura3 leu2 his3 trp1*). Stress tolerance assays were performed using the YNBura⁺ + Galactose 2% solid medium in the presence or not of NaCl (0.5 M), H₂O₂ (4 μM), mannitol (1.2 M) and LiCl (0.05 M). Heat stress assay was performed in water bath at 48 °C for 6 h. Then tenfold serial dilutions were prepared (10⁻¹ to 10⁻³) and spotted on (5 μl) per drop onto these media and incubated at 30 °C for 5 days. The percentage of viable cells was done as previously described by Tounsi et al., (2019).

2.6. Overexpression, purification and stress response analysis of *TmMnSOD* in *Escherichia coli*

The *TmMnSOD* ORF harboring *Bam*HI and *Eco*RI sites was cloned into the pET28a expression vector. The recombinant vector (pET28a-*TmMnSOD*) was transformed into *E. coli* BL21 (DE3) cells for expression. The transformed *E. coli* were grown at 37 °C in LB medium containing 50 μg/ml kanamycin until OD₆₀₀ reached 0.6. The production of recombinant protein was induced by 1 mM isopropyl β-D-thiogalactopyranoside (IPTG) for 4 h at 37 °C. Recombinant protein was purified by affinity chromatography on nickel columns (His60 Ni Superflow Resin Clontech). Purity of target protein was analyzed on 12% SDS-PAGE. *TmMnSOD* activity was performed as described previously by Feki et al. (2016), using increasing amount (25, 50 and 200 μg) of protein of purified recombinant protein with 50 mM potassium phosphate buffer (pH 7.8), 0.1 mM EDTA, 13 mM methionine, 2 μM riboflavin and 75 μM NBT (Nitroblue tetrazolium). The reaction was measured spectrophotometrically at 560 nm. Effects of heavy metals stresses on the growth of *E. coli* cells transformed with recombinant vector (pET28a-*TmMnSOD*) or empty vector were analyzed using spot assay under different treatments with MnCl₂, CdCl₂, CuSO₄, AlCl₃ or ZnSO₄. *E. coli* cells were grown as mentioned above and diluted to 0.6 OD₆₀₀. For spot assay, 5 μL of each sample diluted to 10⁻³ and 10⁻⁴, 10⁻⁵, 10⁻⁶, were spotted on LB plates containing 750 μM of MnCl₂, CdCl₂, CuSO₄, AlCl₃ or ZnSO₄. All these plates were incubated at 37 °C for overnight and photographed.

2.7. Isolation of *TmMnSOD* and *TdMnSOD* promoter regions

The promoter sequence of *TmMnSOD* and *TdMnSOD* were isolated using the high-efficiency thermal asymmetric interlaced (HE-TAIL) PCR

method (Michiels et al., 2003). The genomic DNA of *T. monococcum* and *T. durum* was extracted as previously described by Das et al. (1990). Since the two genes *TmMnSOD* and *TdMnSOD* share more than 90% of identity, four specific reverse primers G1 (5'-GCCGCCGTTGAACTGATGGCGC-3'), G2 (5'-CGTCGAGCTGCTCGAGCGCCTT-3'), G3 (5'-GGGAGGTCGGGGAGCGTGAACGT-3') and G4 (5'-CGGCCAACGTGCGGAGCGCCAT-3') were designed for both genes, in combination with four random primers R1 (5'-NGTCGASWGANAWGAA-3'), R2 (5'-GTNCGASWCANAWGTT-3'), R3 (5'-WGTGNAGWANCANAGA -3') and R4 (5'-NCAG CTWSCNTNTSCTT-3'). Target bands were identified, ligated into the pGEM-T Easy and sequenced.

3. Results

3.1. *TmMnSOD* isolation and sequence analysis

The coding region of *TmMnSOD* was isolated from *T. monococcum* plant treated with medium concentration of NaCl during 2 days. Sequence analysis revealed that the open reading frame (ORF) of *TmMnSOD* (accession number, MK091461) is 699 bp encoding a protein of 232 amino acids with a predicted molecular weight (MW) of 25 kDa and a calculated isoelectric point (PI) of 7.89. The phylogenetic relationships were analyzed between *TmMnSOD* and other plant SOD proteins from wheat, rice, *Brachypodium distachyon*, *Sorghum bicolor* and *Arabidopsis thaliana*. As illustrated in Fig. 1, the identified *TmMnSOD* protein was clearly shown to be related to MnSOD subfamily, sharing high sequence identity (> 80%) with *T. turgidum* *TdMnSOD*, *T. aestivum* *TaMnSOD*, *T. urartu* *TuMnSOD*, *B. distachyon* *BdMSD*, *O. sativa* *OsMSD*, *S. bicolor* *SbSOD6* and *A. thaliana* *AtMSD1*. Protein sequence analysis displayed that *TmMnSOD* was very close to its homolog *TdMnSOD* from durum wheat and was slightly longer by seven amino acids (Supplementary Fig. S1).

Furthermore, we identified the conserved domains of *TmMnSOD* using the InterPro and Pfam tools. These domains are the iron/manganese superoxide dismutase alpha-hairpin domain (Pfam: 00081) and iron/manganese superoxide dismutase C-terminal domain (Pfam: 02777), which are highly conserved in plant MnSOD proteins (Fig. 2A and B). To further compare the structural feature of *TmMnSOD* with their homologs, conserved protein motifs were analyzed using MEME program. As shown in Fig. 2C, a total of eight motifs were identified in all MnSOD proteins. Among them, motif 1 and motif 2 are related to iron/manganese SOD domains. Interestingly, the motif 2 contains the conserved metal-binding domain (DVWEHAYY) of the Mn-SODs.

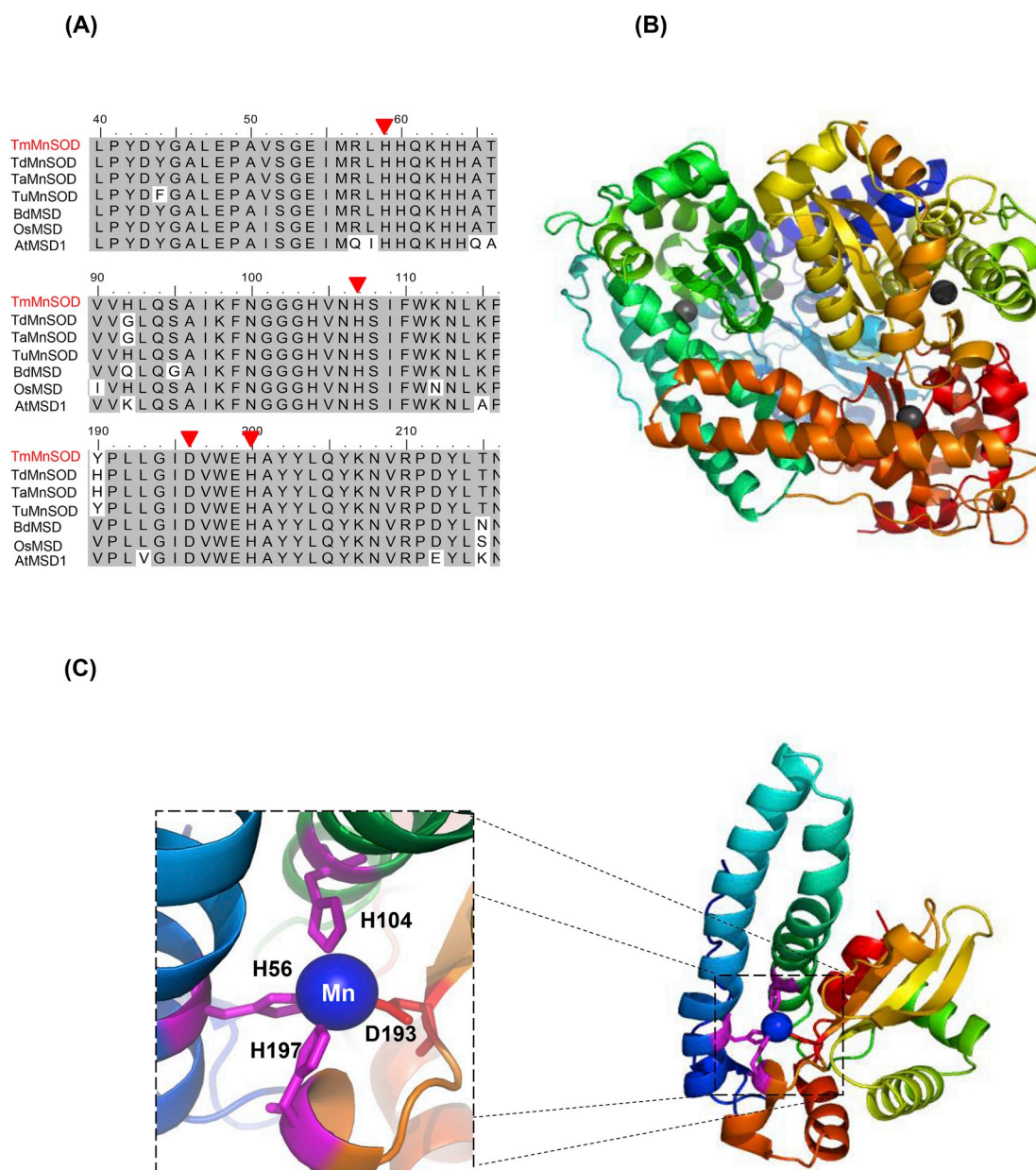


Fig. 4. Sequence analysis and three-dimensional structure of TmMnSOD. (A) Protein sequence alignment of TmMnSOD with *T. durum* TdMnSOD, *T. aestivum* TaMnSOD, *T. urartu* TuMnSOD, *O. sativa* OsMSD, *B. distachyon* BdMSD and *A. thaliana* AtMSD1 to identify the conserved amino acid implicated in Mn ion interaction. The four conserved residues (His56, His104, Asp193 and His197) are indicated by red triangles. (B) TmMnSOD tetramer organization showing the presence of four Mn^{2+} ions. (C) Monomer of TmMnSOD showing the residues His56, His104, Asp193 and His197 implicated in Mn ion interaction. (For interpretation of the references to color in this figure legend, the reader is referred to the Web version of this article.)

Moreover, using CELLO prediction tool, the protein TmMnSOD is potentially localized in the mitochondria (Supplementary Fig. S2).

In addition, the analysis of exon-intron organizations of *TmMnSOD* with *MnSOD* from other plant species revealed the high conservation of exon length and exon-intron numbers. As indicated in Fig. 3, all *MnSOD* members contained 6 exons and 5 introns.

3.2. Prediction of 3D-structure of *TmMnSOD*

The putative 3D-structural model of TmMnSOD was predicted using

the crystal structure of *Arabidopsis thaliana* as a template (Marques et al., 2014) since both MnSOD proteins shared about 80% of identity (Fig. 4A). The Ramachandran evaluation of the TmMnSOD model revealed that 97.2% of residues were in the favored region and 2% of residues in the allowed region with no residue in the outlier region. Accordingly, the model was validated and retained. The examination of the model showed that TmMnSOD forms a homotetramer containing four Mn^{2+} ions and each subunit is composed of a predominantly α -helical N-terminal domain and a mixed α/β C-terminal domain (Fig. 4B and C). As illustrated in Fig. 4C, the residues His56, His104, Asp193

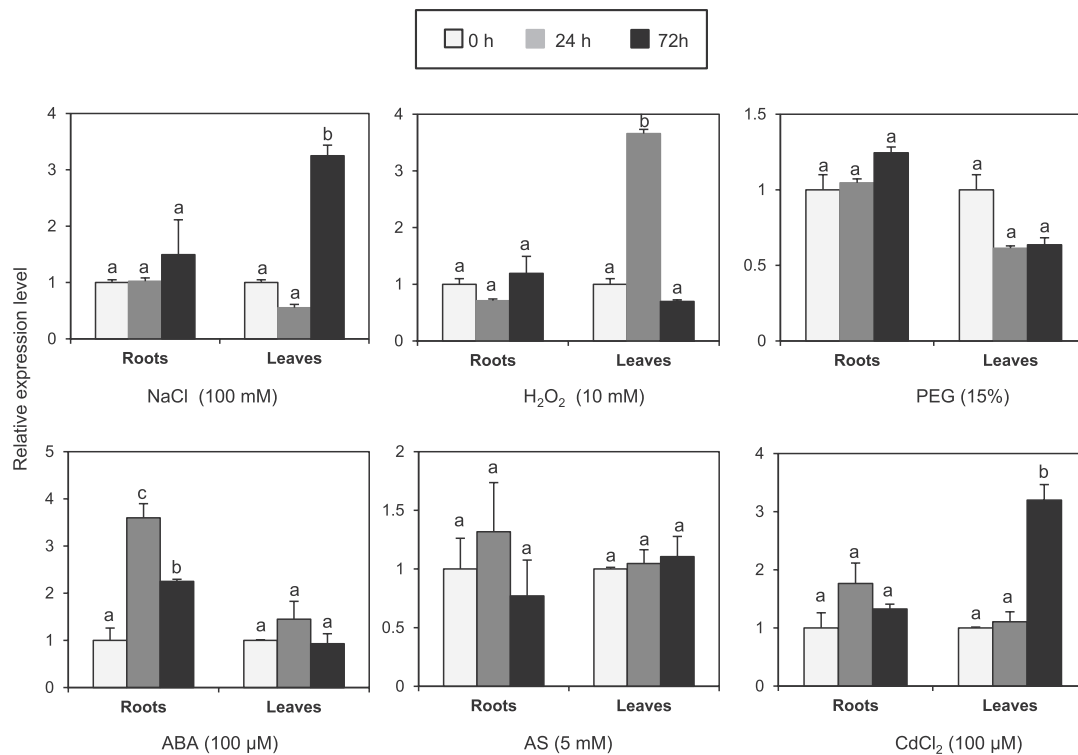


Fig. 5. Expression patterns of *TmMnSOD* in *Triticum monococcum* under various environmental conditions. The expression level of *TmMnSOD* was analyzed after the addition of 100 mM NaCl, 10 mM H₂O₂, polyethylene glycol (PEG) 15%, 100 μM ABA, 5 mM salicylic acid and 100 μM CdCl₂ for 24 and 72 h. Transcript levels are given relative to the average levels in control plants (kept in standard conditions), at the same time. Data are means ± SE of three biological replicates.

and His197 are implicated in Mn ion interaction and form the active site of *TmMnSOD*.

3.3. Expression pattern of *TmMnSOD* under different stress conditions

The expression profile of *TmMnSOD* was analyzed in response to various stress conditions. As indicated in Fig. 5, the expression level of *TmMnSOD* was up-regulated by salt, oxidative and heavy metal stresses in leaves. The transcript level of *TmMnSOD* was increased by a factor close to 3 after 72 h of salt and heavy metal treatments and after 24 h for oxidative stress treatment. In roots, the treatment with 100 μM ABA induced a significant increase in the transcript level of *TmMnSOD*. The expression level of *TmMnSOD* was increased by almost 3 and 2 times after 24 and 72 h of ABA treatment, respectively. On the other hand, the treatments with 15% PEG and 5 mM SA had little effect on *TmMnSOD* expression in roots and leaves.

3.4. Heterologous expression of *TmMnSOD* in yeast cells

To examine the role of *TmMnSOD* under various stress conditions, its overexpression in yeast cells was investigated. As illustrated in Fig. 6A, yeast strains overexpressing *TmMnSOD* and the control strains transformed with the empty vector (pYES2) displayed similar growth under normal condition. In the presence of salt, oxidative, osmotic and heat stresses, the growth rate of *TmMnSOD*-overexpressing yeast cells was improved compared to yeast cells transformed with the empty vector. The number of the recombinant cells was about 8, 1.5 and 2 fold

higher than control cells under H₂O₂, mannitol and heat stresses, respectively. However, in the presence of LiCl in the medium, the number of recombinant cells was similar to the control yeast cells (Fig. 6B). These results suggested that *TmMnSOD* was functional in yeast and able to enhance tolerance to various stresses.

3.5. *TmMnSOD* imparts heavy metal stress tolerance to *E. coli* cells

To investigate whether *TmMnSOD* is involved in response to heavy metals, pET28a-*TmMnSOD* was produced in *E. coli* cells. As indicated in Fig. 7A, the molecular weight (MW) of the purified protein was about 32 KDa. The estimated MW of *TmMnSOD* was 25.3 KDa, and the MW of His6 was about 1 KDa. SOD activity of *TmMnSOD* protein was determined as described by Feki et al., (2016). We clearly showed that this activity increased in the presence of increasing amount of the purified protein (Fig. 7B). Then, the growth of *E. coli* cells overexpressing pET28a-*TmMnSOD* or the empty vector was analyzed in medium containing MnCl₂, CdCl₂, CuSO₄, AlCl₃ and ZnSO₄ (Fig. 7C). Under normal conditions, the growth pattern of recombinant cells was similar to the growth of control cells. By contrast, cells transformed with pET28a-*TmMnSOD* exhibited better growth compared to cells transformed with empty vector in the presence of different heavy metals treatments. These results suggested that *TmMnSOD* could play a potential role in heavy metal stress tolerance.

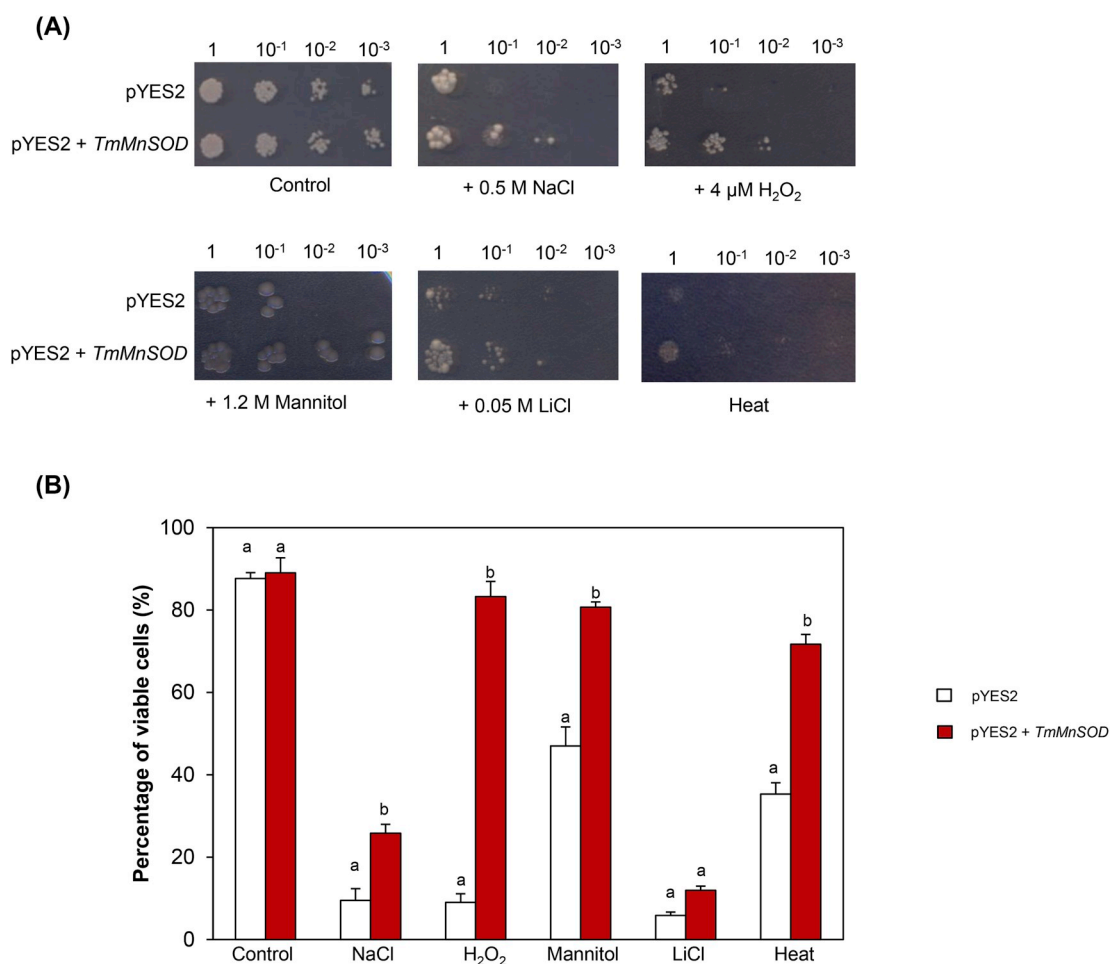


Fig. 6. Functional characterization of *TmMnSOD* expressed in yeast in response to abiotic stress. (A) Yeast cells transformed with the empty vector (pYES2) and with the recombinant vector (pYES2 + *TmMnSOD*) were grown for 5 days under normal growth conditions (YNB-Ura/Gal2%) or after the addition of 0.5 M NaCl, 4 μM H₂O₂, 1.2 M mannitol, 0.05 M LiCl and under heat (48 °C). (B) Presentation of percentage of viable cells under control, salt, oxidative, osmotic, ionic and heat conditions. Data presented are means of at least 3 independent experiments ± S.E. Bars carrying diverse letters are significantly different ($p \leq 0.001$) from each other, according to Duncan test results, while bars carrying the same letters are not significantly different.

3.6. Isolation and *in silico* analysis of *TmMnSOD* and *TdMnSOD* promoters

To gain more knowledge about the regulatory mechanism of wheat MnSOD gene expression, the promoter region of *TmMnSOD* and its homologous *TdMnSOD* from durum wheat were isolated using the thermal asymmetric interlaced PCR (TAIL-PCR) technique. Two promoter sequences, designated as *PrTmMnSOD* (1700 pb) and *PrTdMnSOD* (1971 bp), were identified and verified by sequencing (Fig. 8). The promoter sequence of *TmMnSOD* and *TdMnSOD* were deposited in GenBank with the accession number MK091462 and MK091463, respectively. The 1700 bp DNA sequence upstream the translation initiation codon of *TmMnSOD* and *TdMnSOD* was analyzed using PlantCARE and PLACE bioinformatic tools. Two major groups of putative *cis*-regulatory elements involved in hormone signal and abiotic stress responsiveness, were identified in both promoter sequences. As illustrated in Fig. 9, *in silico* analysis revealed that *TmMnSOD* promoter sequence contains several types of stress-responsive regulatory elements such as two ARE elements and five GT1GMSCAM4. Besides, four kinds of hormone-responsive *cis*-acting elements were found in the *PrTmMnSOD* sequence, which are ABRE involved in the abscisic acid responsiveness,

P-box and GARE-motif related to gibberellin-responsive elements, TGACT-motif involved in the MeJA-responsiveness and TGA-element related to auxin-responsive element. This analysis also revealed the presence of other *cis*-acting regulatory elements, viz. CCGTCC-box and CGCGBOXAT related to meristem specific activation and calmodulin-binding/CGCG box DNA-binding protein, respectively.

Compared with the promoter sequence of *TdMnSOD* from durum wheat, *PrTmMnSOD* sequence contains the highest number of ACGTATERD1 (early responsive elements in dehydration), LTR (involved in low-temperature responsiveness) and CGCGBOXAT (calmodulin-binding/CGCG box DNA-binding protein). However, *PrTdMnSOD* has a great number of the salt and pathogen-responsive GT1GMSCAM4-motif suggesting that the expression level of this gene could be strongly modulated under salt stress condition (Fig. 9). Taken together, this analysis indicated that the expression of *TmMnSOD* and *TdMnSOD* genes are tightly regulated by environmental conditions, in particular by abiotic stress and hormonal signaling, suggesting that despite the high level of sequence identity, these two genes might play distinct roles in plant.

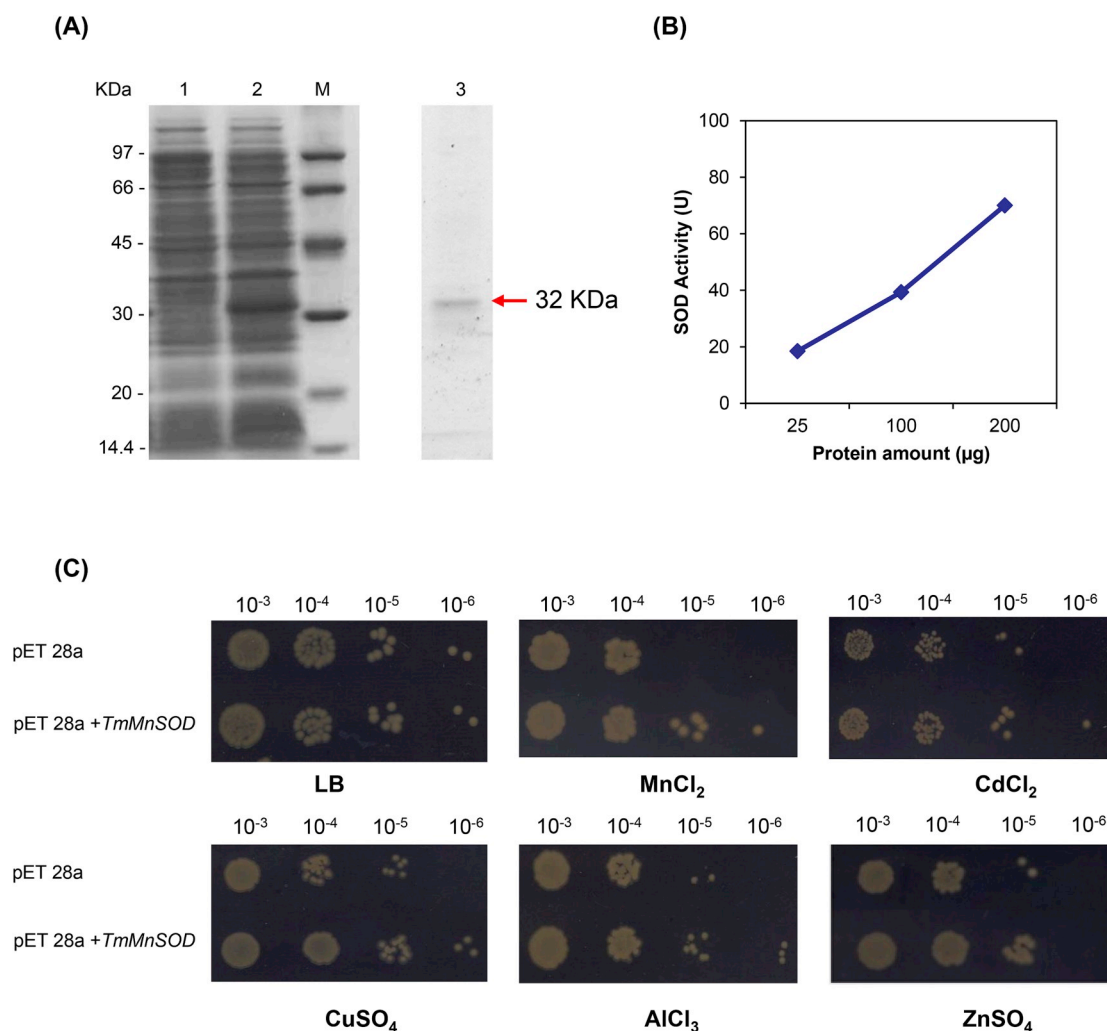


Fig. 7. Effect of Mn, Cd, Cu, Al and Zn stress on the growth of *E. coli* cells overexpressing *TmMnSOD*. (A) SDS-PAGE analysis of *TmMnSOD* overexpression in *E. coli* cells before (lane 1) and after (lane 2) IPTG induction. The arrow indicates the purified His-tagged *TmMnSOD* protein (lane 3) and Marker (M). (B) Determination of specific activity of *TmMnSOD* protein using increasing amount (25, 100 and 200 µg) of the purified protein. (C) Spot assays of BL21 + pET 28a-*TmMnSOD* and BL21 + pET28a on LB plates containing MnCl₂, CdCl₂, CuSO₄, AlCl₃ and ZnSO₄. Five microliters from 10⁻³ to 10⁻⁶ dilutions were spotted onto LB basal plates (control) or supplemented with 750 µM of MnCl₂, CdCl₂, CuSO₄, AlCl₃ or ZnSO₄.

4. Discussion

Abiotic stress including salinity, drought, temperature and heavy metals displays a negative effect on plant growth and productivity of crops in several regions of the world (Mhamdi et al., 2012; Caverzan et al., 2016; He et al., 2018). In response to these adverse conditions, plants have evolved a number of intricate mechanisms to protect their cellular activities and maintain their growth. These mechanisms include the regulation of ROS homeostasis, which is controlled by several enzymatic antioxidants including superoxide dismutase and catalase. SODs are considered as the most efficient scavengers of ROS (Alscher et al., 2002; He et al., 2018). These metallo-enzymes catalyze the dismutation of superoxide anion radical (O₂⁻), generated during plant growth and under different stresses by converting it to hydrogen peroxide (H₂O₂) and oxygen. SOD family from different plant species has been shown to play a crucial role in plant stress tolerance (Mittler, 2002; Faize et al., 2012; Gill et al., 2015; Feki et al., 2016; Wang et al.,

2016; Guan et al., 2017; Sanyal et al., 2018). In wheat, three *MnSOD* genes have been identified based on southern blot analysis (Kumar et al., 2013). However, their specific role in plants is still largely unknown. In the present study, a novel *TmMnSOD* gene from *Triticum monococcum* was identified and functionally characterized. Despite this protein is slightly longer than TdMnSOD, it is very close to MnSOD family from different plants like wheat, rice, *Brachypodium distachyon*, *Sorghum bicolor* and *Arabidopsis thaliana* (Fig. 1). Moreover, like other MnSOD proteins, *TmMnSOD* contains two conserved domains, which are the iron/manganese superoxide dismutase alpha-hairpin domain and iron/manganese superoxide dismutase C-terminal domain (Feki et al., 2016; Wang et al., 2016; Yadav et al., 2018) (Fig. 2). To gain further insights into the protein feature of *TmMnSOD*, its 3-Dimensional structure was generated using the crystal structure of *Arabidopsis thaliana* as a template (Marques et al., 2014). In fact, *TmMnSOD* displays homotetramer subunit organization, incorporating four Mn²⁺ ions. The Mn ion interaction implicates four residues which are His56,

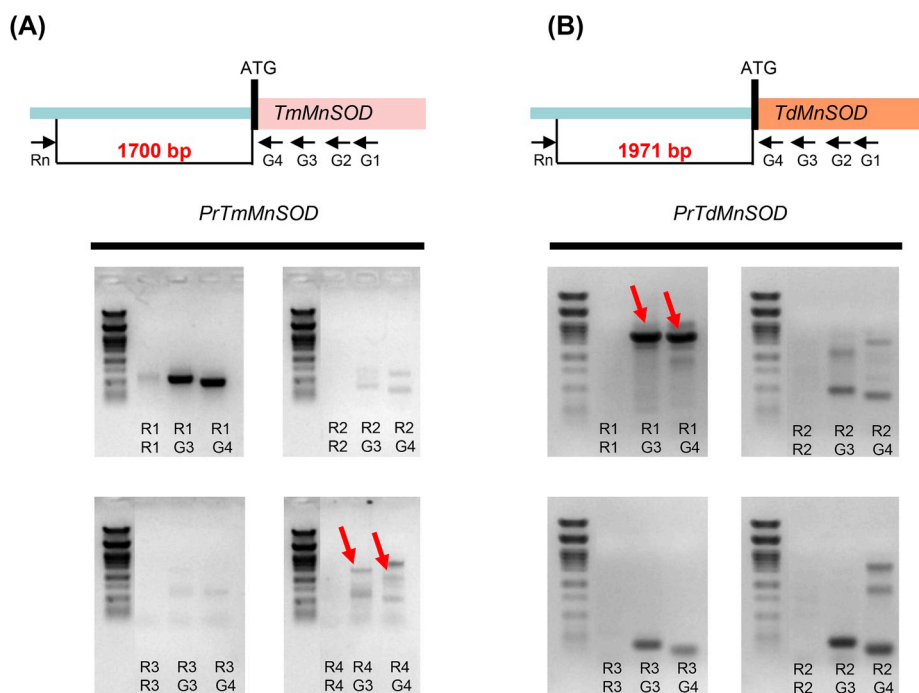


Fig. 8. Isolation of *TmMnSOD* and *TdMnSOD* promoter regions by HE-TAIL-PCR technique. (A) The putative promoter region of *TmMnSOD* (1700 bp) was identified using G3/R4 and G4/R4 primers. (B) The putative promoter region of *TdMnSOD* (1971 bp) was identified using G3/R1 and G4/R1 primers. Target bonds were cloned in pGEM-T EASY vector and then sequenced. The gene specific (G1–G4) and random primers (R1–R4) are marked at the bottom. M: lambda *Pst*I molecular weight marker.

His104, Asp193 and His197, forming the active site of *TmMnSOD* (Fig. 4A and B). Moreover, *TmMnSOD* contains mainly alpha helices with three beta sheets (Fig. 4C), like *TdMnSOD* from *T. durum* (Feki et al., 2016). This organization is in accordance with the analysis of Dehury et al. (2012a,b) showing the dominance of α -helices in the MnSOD structures. These results suggested that *TmMnSOD* is a manganese superoxide dismutase, sharing similar structural features with MnSODs from other plant species.

Based on their metal co-factor, SODs are broadly divided into three groups viz, copper–zinc SOD (Cu/ZnSOD), Iron SOD (FeSOD) and manganese SOD (MnSOD). Cu/ZnSODs were considered as the most abundant isoforms in plants and generally localized in the cytosol, chloroplast and peroxisomes. On the other hand, FeSOD and MnSOD were predominantly found in chloroplast and mitochondria, respectively. In bread wheat, it was reported that TaSOD2 is localized in the cytoplasm contrary to its ortholog AtCSD3, which is strongly accumulated in the peroxisomes (Wang et al., 2016). Concerning *TmMnSOD*, it is potentially localized in the mitochondria, like other MnSOD from different plant species.

So far, it was reported in many studies that MnSOD proteins play a crucial role in response to both biotic and abiotic stresses, and their expression levels change in plant cells depending to the type of stress (Filiz and Tombuloglu, 2015; Feki et al., 2017; Wang et al., 2016; Zhou et al., 2017; Yadav et al., 2018). For example, the expression of the two genes *OsMSD1* and *AtMSD1* was up-regulated in response to salt, drought, cold and heat stresses (Yadav et al., 2018). By contrast, in bread wheat, *TaSOD* was strongly expressed in response to high temperature conditions (Kumar et al., 2013). It is interesting to notice that the expression of *TmMnSOD* was enhanced not only by salt and osmotic stresses like *TdMnSOD* (Feki et al., 2016), but also it was significantly induced in leaves by heavy metal stress. Furthermore, the induction was also obtained in roots exposed to ABA treatment.

To gain insight into the role of *TmMnSOD* in response to various

abiotic stresses, it was overexpressed in yeast cells that were exposed to different stresses. In concordance with *TdMnSOD* from durum wheat (Feki et al., 2016), *TmMnSOD* imparts tolerance to salt, H_2O_2 , mannitol and heat stresses except LiCl stress. Taken together, we suggested that *TmMnSOD* is functional and plays a key role in response to these abiotic stresses. In parallel, *TmMnSOD* is able also to improve tolerance of *E. coli* cells exposed to different heavy metals, which are among the most important factors leading to the generation of reactive oxygen species (ROS) in plants. Several studies indicated the relevant role of antioxidant system in heavy metal stress tolerance (Basu et al., 2001; Yusuf et al., 2012; Singh et al., 2013, 2016; Tiwari and Lata, 2018). It was reported that numerous non-enzymatic antioxidants including glutathione and α -tocopherol enhance heavy metal stress tolerance (Singh et al., 2016). Furthermore, the activities and the expression level of several enzymatic antioxidants such as SOD, CAT and APX were found to be modulated in response to heavy metal toxicity (Basu et al., 2001; Singh et al., 2013; Bharwana et al., 2013; Bashri and Prasad, 2015). Interestingly, *TmMnSOD* from *T. monococcum* ameliorates the growth of *E. coli* cells exposed to Mn, Cd, Cu, Al and Zn treatments suggesting that *TmMnSOD* might play a key role in response to heavy metal stress. Thus, these results can pave the way to future analysis of the role of *TmMnSOD* in transgenic plant under heavy metal conditions.

In wheat, *SOD* genes have been shown to play important roles in plant adaptation to different stresses (Kumar et al., 2013; Wang et al., 2016; Feki et al., 2016). However, the regulatory mechanism that controls their specific functions is still largely unclear. So, the two promoter sequences of *TmMnSOD* and *TdMnSOD* were isolated using the thermal asymmetric interlaced PCR (TAIL-PCR) technique from *T. monococcum* and *T. durum*, respectively (Fig. 8). These two 5'-flanking regions of the two *MnSOD* genes were analyzed and compared in order to identify the transcription factors and *cis*-acting regulatory elements that regulate the expression of *MnSOD* genes in diploid wheat and durum wheat. The analysis showed that the promoters of both genes

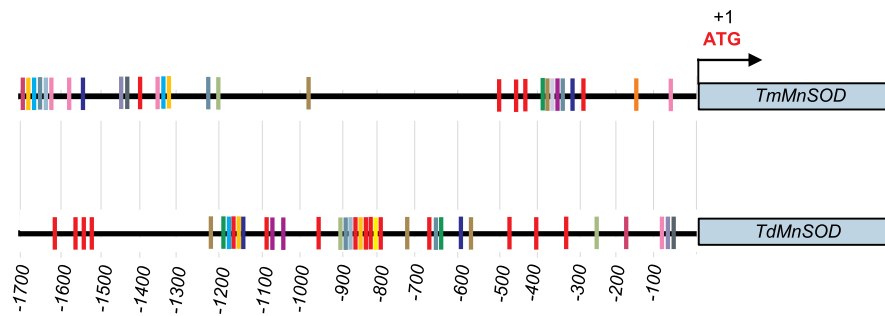


Fig. 9. Schematic representation of putative cis-element sites present in the first 1700 bp of *TmMnSOD* and *TdMnSOD* promoter regions. The search for cis-regulatory elements was performed using PlantCARE and PLACE databases. The position of each motif on promoter is presented with respect to the translation start site (ATG, position 0), marked by an arrow. The promoter of both genes contains putative cis-regulatory elements which may be involved in the regulation of gene expression under various stresses (ARE, PALBOXAPC, GT1GMSCAM4, ABRERATCAL, ACGTATERD1, LTR, MBS and WBOXNTERF3) and hormonal signaling conditions (ABRE, P-box, GARE-motif, TGACT-motif and TCA-element). Other elements putatively related to the meristem specific activation and calmodulin-binding/CGCG box DNA-binding protein, were found in both promoter regions. Identified cis-regulatory motifs were presented in the figure with different colors. The approximate position of the motifs could be identified using the scale provided below. (For interpretation of the references to color in this figure legend, the reader is referred to the Web version of this article.)

	color	Motif	Function	<i>TmMnSOD</i>	<i>TdMnSOD</i>
Stress	Yellow	ARE	essential for the anaerobic induction	2	2
	Purple	PALBOXAPC	Elicitor or light-mediated PAL gene activation	1	1
	Red	GT1GMSCAM4	Pathogen and salt-induced gene	5	15
	Light Blue	ABRERATCAL	Early responsive elements in dehydration	1	1
	Dark Blue	ACGTATERD1	Early responsive elements in dehydration	3	2
	Light Cyan	LTR	involved in low-temperature responsiveness	2	1
	Pink	MBS	MYB binding site involved in drought-inducibility	1	2
	Light Purple	WBOXNTERF3	Wounding responsive element	1	1
	Light Green	CURECORECR	Copper-responsive element	2	3
Hormones	Dark Green	ABRE	involved in the abscisic acid responsiveness	1	2
	Light Green	P-box	gibberellin-responsive element	1	2
	Light Purple	GARE-motif	gibberellin-responsive element	1	-
	Dark Blue	TGACT-motif	involved in the MeJA-responsiveness	2	2
	Orange	TGA-element	auxin-responsive element	1	-
	Yellow	TCA-element	involved in salicylic acid responsiveness	-	1
Others	Dark Grey	CCGTCC-box	related to meristem specific activation	1	1
	Pink	CGCGBOXAT	Calmodulin-binding/CGCG box DNA-binding protein	4	1

contain putative cis-regulatory elements that are involved in the regulation of gene expression under abiotic stress and hormonal signaling conditions (Fig. 9). Interestingly, various cis-acting elements are present in these two promoter regions, which are involved essentially in biotic and abiotic stresses. It is worth to notice that the numbers of these elements in the two promoter regions are very close, except the element involved in pathogen and salt induced genes. In fact, the promoter region of *TmMnSOD* harbored an important number of GT1GMSCAM4 motifs, which may explain the prominent induction of this gene under salt stress condition (Figs. 5 and 9). Therefore, our results suggest that *TmMnSOD* gene could be considered as attractive target for improvement of salt tolerance of wheat.

5. Conclusion

In summary, a novel mitochondrial MnSOD was identified from *T. monococcum*. We clearly showed that the expression level of *TmMnSOD* was up-regulated in response to various stresses. Furthermore, *TmMnSOD* was able to enhance yeast and *E. coli* cells growth under abiotic stresses and heavy metal toxicity. The presence of several cis-regulatory elements in the promoter region of both *TmMnSOD* and *TdMnSOD* might evince that these two corresponding genes are promising candidates for improving abiotic stress tolerance in wheat.

Conflicts of interest

The authors declare that they have no conflict of interest.

Author's contribution

ST, KF and FB conceived and designed the experimental plan. ST, YK, CA and MG performed the experiments and wrote the manuscript. ST, SJ, MNS, KF and FB analyzed the data and revised the manuscript. All the authors agreed on the contents of the paper and post no conflicting interest.

Acknowledgements

This study was supported by a grant from the Ministry of Higher Education and Scientific Research, Tunisia.

Appendix A. Supplementary data

Supplementary data to this article can be found online at <https://doi.org/10.1016/j.plaphy.2019.08.001>.

References

- Abu Romman, S., Shatnawi, M., 2010. Isolation and expression analysis of chloroplastic copper/zinc superoxide dismutase gene in barley. *South Afr. J. Bot.* 77, 328–334.
- Alscher, M.G., Erturk, N., Heath, L.S., 2002. Role of superoxide dismutases (SODs) in controlling oxidative stress in plants. *J. Exp. Bot.* 53, 1331–1341.
- Bashri, G., Prasad, S.M., 2015. Indole acetic acid modulates changes in growth, chlorophyll a fluorescence and antioxidant potential of *Trigonella foenum-graecum* L. grown under cadmium stress. *Acta Physiol. Plant.* 37, 1745.
- Basu, U., Good, A.G., Taylor, G.J., 2001. Transgenic *Brassicanapus* plants overexpressing aluminium-induced mitochondrial manganese superoxide dismutase cDNA are resistant to aluminium. *Plant Cell Environ.* 24, 1278–1269.
- Bharwana, S.A., Ali, S., Farooq, M.A., Iqbal, N., Abbas, F., Ahmad, M.S.A., 2013. Alleviation of lead toxicity by silicon is related to elevated photosynthesis, anti-oxidant enzymes suppressed lead uptake and oxidative stress in cotton. *J. Bioremed. Biodegrad.* 4, 4.
- Caverzan, A., Casassola, A., Brammer, S.P., 2016. Antioxidant responses of wheat plants under stress. *Genet. Mol. Biol.* 39, 1–6.
- Das, O.P., Alvarez, C., Chaudhuri, S., Messing, J., 1990. Molecular methods for genetic analysis of maize. *Methods Mol. Cell. Biol.* 1, 213–222.
- Davenport, R., James, R.A., Zakrisson-Plogander, A., Tester, M., Munns, R., 2005. Control of sodium transport in durum wheat. *Plant Physiol.* 137, 807–818.
- Dehury, B., Sarma, K., Sarmah, R., Sahu, J., Sahoo, S., Sahu, M., Sen, P., Modi, K.M., Barooah, M., 2012a. *In silico* analyses of superoxide dismutases (SODs) of rice (*Oryza sativa* L.). *J. Plant Biochem. Biotechnol.* 22, 150–156.
- Dehury, B., Sarma, K., Sarmah, R., Sahu, J., Sahoo, S., Sahu, M., Sen, P., Modi, K.M., Barooah, M., 2012b. *In silico* analyses of superoxide dismutases (SODs) of rice (*Oryza sativa* L.). *J. Plant Biochem. Biotechnol.* 22, 150–156.
- Del Rio, L.A., Sandalio, L.M., Altomare, D.A., Zilinskas, B.A., 2003. Mitochondrial and peroxisomal manganese superoxide dismutase: differential expression during leaf senescence. *J. Exp. Bot.* 54, 923–933.
- Faize, M., Burgos, L., Faize, L., Petri, C., Barba-Espin, G., Diaz-Vivancos, P., Clemente-Moreno, M.J., Alburquerque, N., Hernández, J.A., 2012. Modulation of tobacco bacterial disease resistance using cytosolic ascorbate peroxidase and Cu, Zn-superoxide dismutase. *Plant Pathol.* 61, 858–866.
- Feki, K., Farhat-Khemakhem, A., Kamoun, Y., Saibi, W., Gargouri, A., Brini, F., 2016. Responses of transgenic Arabidopsis plants and recombinant yeast cells expressing a novel durum wheat manganese superoxide dismutase TdMnSOD to various abiotic stresses. *J. Plant Physiol.* 198, 56–68.
- Feki, K., Tounsi, S., Brini, F., 2017. Comparison of antioxidant system in tolerant and susceptible wheat seedling in response to salt stress. *Span. J. Agric. Res.* 15 (4).
- Filiz, E., Tombuloglu, H., 2015. Genome-wide distribution of superoxide dismutase (SOD) gene families in *Sorghum bicolor*. *Turk. J. Biol.* 39, 49–59.
- Gietz, R.D., Schiestl, R.H., Willems, A.R., Woods, R.A., 1995. Studies on the transformation of intact yeast cells by the LiAc/SS-DNA/PEG procedure. *Yeast* 11, 355–360.
- Gill, S.S., Tuteja, N., 2010. Reactive oxygen species and antioxidant machinery in abiotic stress tolerance in crop plants. *Plant Physiol. Biochem.* 48, 909–930.
- Gill, S.S., Anjum, N.A., Gill, R., Yadav, S., Hasanuzzaman, M., Fujita, M., Mishra, P., Sabat, S.C., Tuteja, N., 2015. Superoxide dismutase - mentor of abiotic stress tolerance in crop plants. *Environ. Sci. Pollut. Res. Int.* 22, 10375–10394.
- Guan, Q., Liao, X., He, M., Li, X., Wang, Z., Ma, H., Yu, S., Liu, S., 2017. Tolerance analysis of chloroplast *Oscu/Zn-SOD* overexpressing rice under NaCl and NaHCO₃ stress. *PLoS One* 12, e186052.
- He, M., He, C.H., Ding, N.Z., 2018. Abiotic stresses: general defenses of land plants and chances for engineering multistress tolerance. *Front. Plant Sci.* 9, 1771.
- Higo, K., Ugawa, Y., Iwamoto, M., Korenaga, T., 1999. Plant *cis*-acting regulatory DNA elements (PLACE) database. *Nucleic Acids Res.* 27, 297–300.
- Khan, N.A., Samiullah Singh, S., Nazar, R., 2007. Activities of antioxidative enzymes, sulphur assimilation, photosynthetic activity and growth of wheat (*Triticum aestivum*) cultivars differing in yield potential under cadmium stress. *J. Agron. Crop Sci.* 193, 435–444.
- Kliebenstein, D.J., Monde, R., Last, R.L., 2010. Superoxide dismutase in *Arabidopsis*: an eclectic enzyme family with disparate regulation and protein localization. *Plant Physiol.* 118, 637–650.
- Kumar, R.R., Sharma, S.K., Goswami, S., Singh, K., Gadpayle, K.A., Singh, G.P., Pathak, H., Rai, R.D., 2013. Transcript profiling and biochemical characterization of mitochondrial superoxide dismutase (mtSOD) in wheat (*Triticum aestivum*) under different exogenous stresses. *Aust. J. Crop. Sci.* 7, 414–424.
- Lescot, M., Déhais, P., Thijs, G., Marchal, K., Moreau, Y., Van de Peer, Y., Rouzé, P., Rombauts, S., 2002. PlantCARE, a database of plant *cis*-acting regulatory elements and a portal to tools for *in silico* analysis of promoter sequences. *Nucleic Acids Res.* 30, 325–327.
- Livak, K.J., Schmittgen, T.D., 2001. Analysis of relative gene expression data using real-time quantitative PCR and the 2^{-DDCT} method. *Methods* 25, 402–408.
- Marques, A.T., Santos, S.P., Rosa, M.G., Rodrigues, M.A.A., Abreu, J.A., Frazao, C., Romao, C.V., 2014. Expression, purification and crystallization of MnSOD from *Arabidopsis thaliana*. *Acta Crystallogr.* 70, 669–672.
- Mhamdi, A., Queval, G., Chaouch, S., Vanderauwera, S., Van Breusegem, F., Noctor, G., 2010. Catalase function in plants: a focus on Arabidopsis mutants as stress-mimic models. *J. Exp. Bot.* 61, 4197–4220.
- Mhamdi, A., Noctor, G., Baker, A., 2012. Plant catalases: peroxisomal redox guardians. *Arch. Biochem. Biophys.* 525, 181–194.
- Michiels, A., Tucker, M., Van den Ende, W., Van Laere, A., 2003. Chromosomal walking of flanking regions from short known sequences in GC-rich plant genomic DNA. *Plant Mol. Biol. Report.* 21, 295–302.
- Miller, A.F., 2012. Superoxide dismutases: ancient enzymes and new insights. *FEBS Lett.* 586, 585–595.
- Mittler, R., 2002. Oxidative stress, antioxidants and stress tolerance. *Trends Plant Sci.* 7, 405–410.
- Nath, K., Kumar, S., Poudyal, R.S., Yang, Y.N., Timilsina, R., Park, Y.S., Nath, J., Chauhan, P.S., Pant, B., Lee, C.H., 2014. Developmental stagedependent differential gene expression of superoxide dismutase isoenzymes and their localization and physical interaction network in rice (*Oryza sativa* L.). *Genes. Genom* 36, 45–55.
- Sanyal, R.P., Samant, A., Prashar, V., Sharan Misra, H., Saini, A., 2018. Biochemical and functional characterization of OsCSD3, a novel CuZn superoxide dismutase from rice. *Biochem. J.* 475, 3105–3121.
- Singh, V.P., Srivastava, P.K., Prasad, S.M., 2013. Nitric oxide alleviates arsenic-induced toxic effects in ridged Luffa seedlings. *Plant Physiol. Biochem.* 71, 155–163.
- Singh, S., Parihar, P., Singh, R., Singh, V.P., Prasad, S.M., 2016. Heavy metal tolerance in plants: role of transcriptomics, proteomics, metabolomics, and ionomics. *Front. Plant Sci.* 6, 1143.
- Song, J., Zeng, L., Chen, R., Wang, Y., Zhou Yong, Z., 2018. *In silico* identification and expression analysis of superoxide dismutase (SOD) gene family in *Medicago truncatula*. *3 Biotech* 8, 348.
- Tiwari, S., Lata, C., 2018. Heavy metal stress, signaling, and tolerance due to plant-associated microbes: an overview. *Front. Plant Sci.* 9, 452.
- Tounsi, S., Kamoun, Y., Feki, K., Jemli, S., Saïdi, M.N., Ziadi, H., Alcon, C., Brini, F., 2019. Localization and expression analysis of a novel catalase from *Triticum monococcum* TmCAT1 involved in response to different environmental stresses. *Plant Physiol. Biochem.* 139, 366–378.
- Tyagi, S., Sharma, S., Taneja, M., Shumayla Kumar, R., Sembli, J.K., Upadhyay, S.K., 2017. Superoxide dismutases in bread wheat (*Triticum aestivum* L.): comprehensive characterization and expression analysis during development and, biotic and abiotic stresses. *Agri. Gene.* 6, 1–13.
- Verma, D., Lakhpanal, N., Singh, K., 2019. Genome-wide identification and characterization of abiotic-stress responsive SOD (superoxide dismutase) gene family in *Brassica juncea* and *B. rapa*. *BMC Genomics* 20, 227.
- Wang, M., Zhao, X., Xiao, Z., Yin, X., Xing, T., 2016. A wheat superoxide dismutase gene TaSOD2 enhances salt resistance through modulating redox homeostasis by promoting NADPH oxidase activity. *Plant Mol. Biol.* 91, 115–130.
- Yadav, S., Gill, S.S., Passricha, N., Gill, R., Badhwar, P., Anjum, N.A., Francisco, J.B.J., Tuteja, N., 2018. Genome-wide analysis and transcriptional expression pattern-assessment of superoxide dismutase (SOD) in rice and Arabidopsis under abiotic stresses. *Plant Gene* 17, 100165.
- Yusuf, M., Fariduddin, Q., Ahmad, A., 2012. 24-Epi brassinolide modulates growth, nodulation, antioxidant system, and osmolyte in tolerant and sensitive varieties of *Vigna radiata* under different levels of nickel: a shotgun approach. *Plant Physiol. Biochem.* 57, 143–153.
- Zhang, H.N., Li, X.J., Li, C.D., Xiao, K., 2008. Effects of overexpression of wheat superoxide dismutase (SOD) genes on salt tolerant capability in tobacco. *Acta Agron. Sin.* 34, 1403–1408.
- Zhang, J., Li, B., Yang, Y., Hu, W., Chen, F., Xie, L., Fan, L., 2016a. Genomewide characterization and expression profiles of the superoxide dismutase gene family in *Gossypium*. *Int. J. Genom.* 2016 8740901.
- Zhang, J., Li, B., Yang, Y., Hu, W., Chen, F., Xie, L., Fan, L., 2016b. Genome wide characterization and expression profiles of the superoxide dismutase gene family in *Gossypium*. *Int. J. Genom.* 2016 8740901.
- Zhou, Y., Hu, L., Wu, H., Jiang, L., Liu, S., 2017. Genome-wide identification and transcriptional expression analysis of cucumber superoxide dismutase (SOD) family in response to various abiotic stresses. *Int. J. Genom* 2017 7243973.